Division of Pharmaceutics, Faculty of Pharmacy, Rhodes University, Grahamstown, South Africa

Development, manufacture and characterization of niosomes for the delivery for nevirapine

B. A. Witika, R. B. Walker

Received September 13, 2018, accepted November 15, 2018

**Corresponding author: Roderick B. Walker, Division of Pharmaceutics, Faculty of Pharmacy, Rhodes University, Grahamstown, South Africa 6140*
r.b.walker@ru.ac.za

Pharmazie 74: 91–96 (2019) *doi: 10.1691/ph.2019.8168*

Nevirapine (NVP), used for the treatment of HIV/AIDS, exhibits unpredictable oral bioavailability, has a poor side effect profile and requires frequent dosing. Niosomes are novel drug delivery systems that have the potential to overcome these challenges. A thin layer hydration approach was used to produce niosomes and optimisation was undertaken using design of experiments (DoE) and response surface methodology (RSM) establish and identify parameters that may affect the manufacture of niosomes. The impact of cholesterol and surfactant content, hydration time and temperature on manufacture was investigated. Critical quality attributes (CQA) in respect of particle size (PS), entrapment efficiency (EE), polydispersity index (PDI) and the amount of NVP released at 48 hours was also assessed. The optimised niosome composition was identified and manufactured and the CQA characterised prior to placing the batch on stability for 12 weeks at 4±2 °C and 22±2 °C. The PS, PDI, EE and % NVP released at 48 h was 523.36±23.16 nm, 0.386±0.054, 96.8 % and 25.3 % for niosomes manufactured with Span® 20. Similarly, the parameters were 502.87±21.77 nm and 0.394±0.027, 98.0 % and 25.0 % for mean PS, PDI, EE and %NVP released at 48 h for Span® 80 niosomes. All characterisation was undertaken on the day of manufacture. In conclusion, a simple, cheap, rapid and precise method of manufacture of NVP niosomes was developed, validated and optimised using DoE and RSM and the product exhibited the target CQA.

1. Introduction

Currently, the only effective medication for HIV treatment is highly active anti-retroviral therapy (HAART), characterised by the use of more than one of five therapeutic classes including nucleosides/nucleotide reverse transcriptase inhibitors (NRTI), non-nucleoside reverse transcriptase inhibitors (NNRTI), integrase inhibitors (II), protease inhibitors (PI) and fusion inhibitors (FI). The bioavailability of these molecules is relatively low due to hepatic first pass metabolism and therefore frequent dosing is required to achieve therapeutic levels, often resulting in lack of adherence to therapy that may lead to poor clinical outcomes (Govender et al. 2008).

Nevirapine (NVP) is a NNRTI used in combination for the suppression of HIV to halt progression to AIDS (Ofotokun et al. 2007). NNRTI compounds act through non-competitive binding to the non-allosteric site of the reverse transcriptase enzyme. NVP requires frequent dosing and exhibits toxicity including serious side-effects such as skin reactions, Stevens-Johnson Syndrome and liver damage (Stern et al. 2003; Luther and Glesby 2007).

The development and use of liposomes, solid lipid nanoparticles, dendrimers, nanoparticulate powders, nano-suspensions, micelles and microemulsions have revolutionized approaches to enhancing therapy and lipid vesicles offer an attractive option for improving drug delivery (Mayer et al. 1986; Gregoriadis 1995; Uchegbu and Vyas 1998; Torchilin 2007; Shegokar and Singh 2011; Saad et al. 2012; Wilkhu et al. 2014).

The objective of this study was to develop a novel, simple, precise and repeatable approach for the delivery of nevirapine using Span® 20 and 80 and investigate the formation and manufacturability of NVP containing niosomes. In addition factors affecting NVP entrapment, entrapment efficiency, particle size, polydispersity index and release of NVP at 48 h were the Critical Quality Attributes (CQA) investigated. Response surface methodology (RSM) and design of experiments (DoE) was used to optimize NVP formulations.

2. Investigations, results and discussion

2.1. Formulation development

2.1.1. Particle size (PS)

The results obtained revealed a strong correlation between particle size (PS) and cholesterol content. The impact of cholesterol and surfactant content are summarised and depicted in the ANOVA summary (Table 1) with significant results reported in red and the 3D response surface plot (Fig. 1). These data reveal that a synergistic relationship exists between the molar concentration of cholesterol and surfactant used on particle size. The surface plots also reveal that relatively small niosomes are produced when the cholesterol content is low and the surfactant content is constant. These results are consistent with previous findings in which an increase in mean PS with increasing cholesterol content was reported (Gregoriadis and Davis 1979; Azmin et al. 1985; Uchegbu and Duncan 1997; Sezgin-Bayindir and Yuksel 2012; Wilkhu et al. 2014). The mean particle size targeted can therefore be produced by manipulation of the combined effects of cholesterol and surfactant content when manufacturing niosomes.

2.1.2. Polydispersity index (PDI)

The ANOVA results summary (Table 2) listed for the polydispersity index (PDI) revealed that the model was not significant and that none of the factors investigated had a significant effect on PDI.

2.1.3. Entrapment efficiency (EE)

The ANOVA results summary (Table 3) revealed that EE was influenced by cholesterol content. The 3D response surface plot (Fig. 2) depicts the profound impact of cholesterol content on entrapment efficiency and that a linear correlation between cholesterol content and EE existed. The presence of surfactant marginally increases entrapment efficiency. The presence of cholesterol increases the

Table 1: ANOVA data for response surface quadratic model for PS

Source	Sum of squares	Df	Mean square	F value	p-value prob > F
Model	2.00	14	0.14	12.70	< 0.0001
A-Rotation speed	6.396E-003	1	6.396E-003	0.57	0.4633
B-Hydration time	5.168E-004	1	5.168E-004	0.046	0.8334
C-Molar concentration cholesterol	1.34	1	1.34	118.81	< 0.0001
D-Molar concentration surfactant	0.21	1	0.21	18.67	0.0007
AB	2.575E-004	1	2.575E-004	0.023	0.8819
AC	6.802E-003	1	6.802E-003	0.60	0.4497
AD	8.205E-005	1	8.205E-005	7.294E-003	0.9331
BC	0.021	1	0.021	1.84	0.1968
BD	0.017	1	0.017	1.53	0.2358
CD	0.010	1	0.010	0.89	0.3612
A^2	9.850E-004	1	9.850E-004	0.088	0.7716
B^2	0.012	1	0.012	1.08	0.3170
C^2	0.24	1	0.24	21.34	0.0004
D^2	0.024	1	0.024	2.17	0.1630
Residual	0.16	14	0.011		

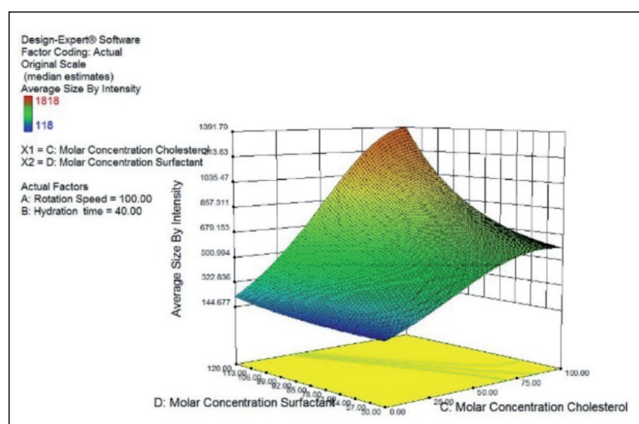

Fig. 1: 3D response surface plot depicting the impact of cholesterol and surfactant content on particle size.

entrapment efficiency by reducing a liquid-gel transition allowing vesicles to incorporate more drug (Yoshioka et al. 1994). The data therefore suggests that to maximise EE an increase in cholesterol content is required to yield high entrapment efficiencies.

Table 2: ANOVA data for response surface 2FI model for PDI

Source	Sum of squares	Df	Mean square	F value	p-value prob > F
Model	0.28	10	0.028	1.58	0.1920
A-Rotation speed	8.234E-003	1	8.234E-003	0.47	0.5026
B-Hydration time	0.037	1	0.037	2.07	0.1669
C-Molar concentration cholesterol	3.830E-006	1	3.830E-006	2.177E-004	0.9884
D-Molar concentration surfactant	0.011	1	0.011	0.60	0.4479
AB	2.155E-003	1	2.155E-003	0.12	0.7304
AC	0.031	1	0.031	1.77	0.1999
AD	0.070	1	0.070	3.99	0.0611
BC	0.10	1	0.10	5.81	0.0269
BD	0.025	1	0.025	1.43	0.2475
CD	6.684E-003	1	6.684E-003	0.38	0.5454
Residual	0.32	18	0.018		

Table 3: ANOVA data for the response surface model for EE

Source	Sum of squares	Df	Mean square	F value	p-value prob > F
Model	490.58	4	122.65	17.11	< 0.0001
A-Rotation speed	0.27	1	0.27	0.037	0.8486
B-Hydration time	0.23	1	0.23	0.032	0.8603
C-Molar concentration of cholesterol	475.78	1	475.78	66.38	< 0.0001
D-Molar concentration of surfactant	14.32	1	14.32	2.00	0.1703
Residual	172.02	24	7.17		

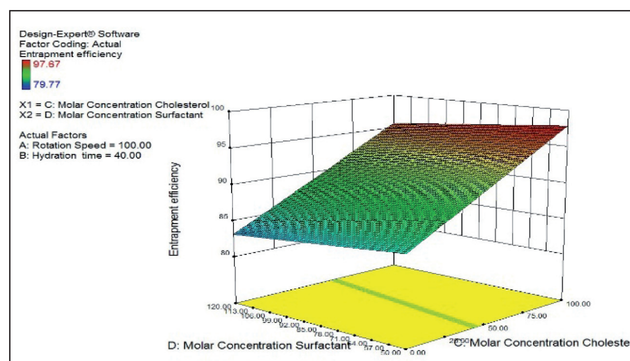

Fig. 2: 3D response surface plot depicting the impact of cholesterol and surfactant content on entrapment efficiency

2.1.4. NVP Released at 48 hours

The 3D response surface plot (Fig. 3) reveals cholesterol and surfactant content as important factors affecting NVP release. Increasing the cholesterol content reduces the rate of NVP release and the presence of increased amounts of surfactant enhanced the release to a maximum when cholesterol was included at low concentration. The extent of NVP release can therefore be modulated by alteration of content to ensure the combined effects of cholesterol and surfactant are realised when manufacturing niosomes.

Table 4: ANOVA data for response surface quadratic model for % NVP released at 48 h

Source	Sum of squares	Df	Mean square	F value	p-value prob > F
Model	1.768E-004	14	1.263E-005	70.46	< 0.0001
A-Rotation speed	1.790E-009	1	1.790E-009	9.983E-003	0.9218
B-Hydration time	2.851E-009	1	2.851E-009	0.016	0.9014
C-Molar concentration cholesterol	1.067E-004	1	1.067E-004	595.14	< 0.0001
D-Molar concentration surfactant	3.907E-005	1	3.907E-005	217.91	< 0.0001
AB	1.197E-008	1	1.197E-008	0.067	0.7998
AC	4.010E-009	1	4.010E-009	0.022	0.8832
AD	2.501E-008	1	2.501E-008	0.14	0.7144
BC	1.082E-007	1	1.082E-007	0.60	0.4501
BD	2.092E-008	1	2.092E-008	0.12	0.7377
CD	9.962E-006	1	9.962E-006	55.57	< 0.0001
A^2	3.159E-007	1	3.159E-007	1.76	0.2056
B^2	1.100E-009	1	1.100E-009	6.139E-003	0.9387
C^2	6.253E-006	1	6.253E-006	34.88	< 0.0001
D^2	7.154E-006	1	7.154E-006	39.90	< 0.0001
Residual	2.510E-006	14	1.793E-007		

2.2. Formulation optimization

A major objective of these studies was to produce stable NVP niosomes capable of controlling and/or sustaining NVP release. A

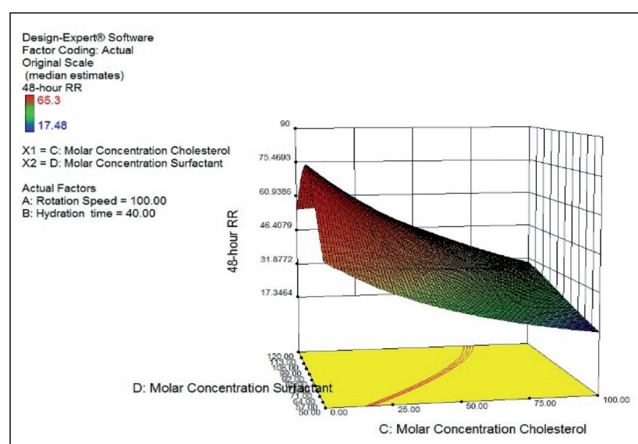

Fig. 3: 3D response surface plot depicting the impact of cholesterol and surfactant content on NVP released at 48 h

numerical optimization approach using Design Expert® software was used to identify the optimum formulation composition and associated process parameters that would lead to the development of a stable niosome formulation with the potential to control and/or sustain the release of NVP. The ZP was maintained at -70±10 mV by adding 5 µmol dihexadecylphosphate (DCP) to ensure the stability of all formulations. The PDI and PS of the formulation monitored to assess the stability of the dispersions. The encapsulation of a large quantity of NVP was necessary to prevent wastage and improve efficiency of the manufacturing process. NVP release over 48 h was used to assess the sustained release characteristics of this technology.

The desirability for the model generated was found to be 0.909 and the optimal conditions were located in the desirability zone. As cholesterol is costly it was decided to maintain the concentration of this excipient at 50 µmol and use a surfactant concentration at 50 µmol. The optimal niosome formulation was manufactured using 50 µmol surfactant viz., Span® 80 or 20 and cholesterol, 5µmol DCP and the process parameters summarized in Table 5.

Table 5: Summary of optimized composition and production conditions

Process variable	Optimised condition
Rotation speed	100 rpm
Rotation time	45 min
Cholesterol content	50 µmol
Surfactant content	50 µmol
DCP	5 µmol
Chloroform	9 ml
Methanol	1 ml
PBS pH 7.4	10 ml

2.2.1. Characterization of optimized NVP niosomes

Differential scanning calorimetry (DSC) was used to investigate potential polymorphism in the optimized NVP niosome formulation and the data are depicted in Fig. 4.

The DSC thermogram reveals a melting endotherm for NVP that is relatively sharp at 235.41 °C. The peaks for cholesterol and DCP were observed at 127.15 °C and 68.98 °C, respectively. All excipients and API appear to maintain crystallinity during the manufacturing process and this is significant in attempting to produce a sustained release formulation that exhibits good stability. The crystalline formulations exhibit low aqueous solubility and improved long term stability when compared to amorphous formulations. A solid drug in the amorphous state exhibits no interactions or bonds in the crystal lattice structure that must be disrupted for the compound to enter solution therefore displaying a higher apparent solubility

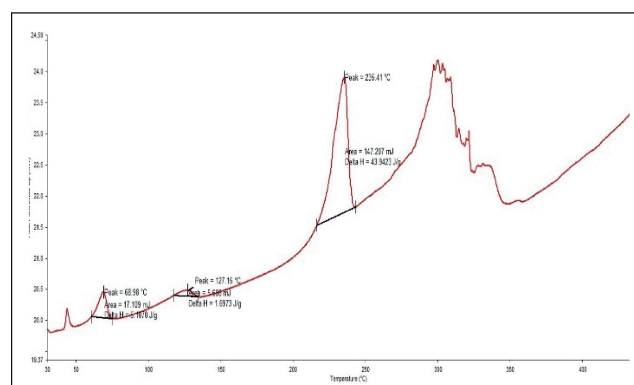

Fig. 4: DSC thermogram of optimized NVP niosomes.

compared to that of crystalline forms of that compound (Hancock and Parks 2000).

X-Ray diffraction (XRD) was used to ascertain the crystallinity of NVP in niosomes. The diffractogram depicted in Fig. 5 reveals the presence of NVP in the niosomes.

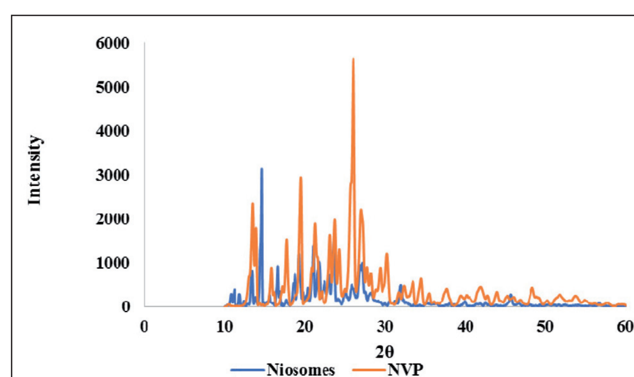

Fig. 5: Diffractogram showing intensity peaks for NVP and NVP loaded niosomes

The diffractogram (Fig. 5) reveals the crystalline nature of the NVP in niosomes. The niosomes were intended for sustained release and as such crystallinity is very important. The most significant peaks for NVP are visible in the NVP niosome albeit with differences in intensities which is due to the manufacturing process resulting in changes in electron density. The maintenance of crystallinity of NVP during manufacturing is important when producing sustained release formulations as crystalline compounds dissolve and diffuse at a slower rate when compared to amorphous materials, in addition to possessing a higher degree of stability with that low solubility (Hancock and Parks 2000).

The stability of niosome dispersions is dependent on a number of factors including PS and PDI. It essential that these CQA are adequately monitored during manufacture and storage. The mean PS and PDI of NVP niosomes manufactured using Span® 20 was 523.36±23.16 nm and 0.386±0.054 determined on the day of manufacture. Similarly, values of 502.87±21.77 nm and 0.394±0.027 for mean PS and PDI were established on the day of manufacture for Span® 80 niosomes. It is clear that Span® 20 and 80 formulations produced niosomes in the nanometer range and the particle size was < 0.500.

However, the PDI value observed for Span® 20 niosomes was greater than that of the Span® 80 niosomes. The larger HLB value of Span® 20 resulted in larger and more polydisperse niosome systems. Therefore, when the amount of NVP in Span® 20 and 80 is constant it is likely that Span® 20 niosomes would exhibit a larger particle size. However, the size of the niosomes may also be affected by formulation variables such as cholesterol and surfactant content. The presence of cholesterol and larger quantities of surfactant showed an increase in PS. This indicates that altering the quantities of cholesterol and surfactant as well as the cholesterol to surfactant ratio can produce niosomes of a particular size.

Transmission Electron Microscopy (TEM) was used to determine the shape and particle size of the niosomes produced using optimized composition and process parameters. The data was generated using the original aqueous solutions prior to lyophilisation of each. A typical TEM of the niosomes is depicted in Fig. 6.

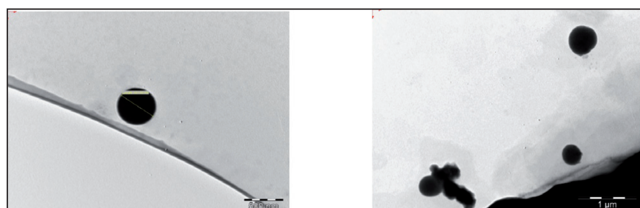

Fig. 6: TEM of an optimized NVP niosome

The data suggest that the niosomes were spherical and were approximately 500 nm in diameter which is consistent with the PS dynamic light scattering (DLS) studies.

Fourier-transform infrared spectroscopy (FTIR) was conducted to ascertain the molecular nature of NVP and all excipients prior to and following processing. The spectrum for NVP niosomes and that of empty niosomes and NVP alone are depicted in Fig. 7.

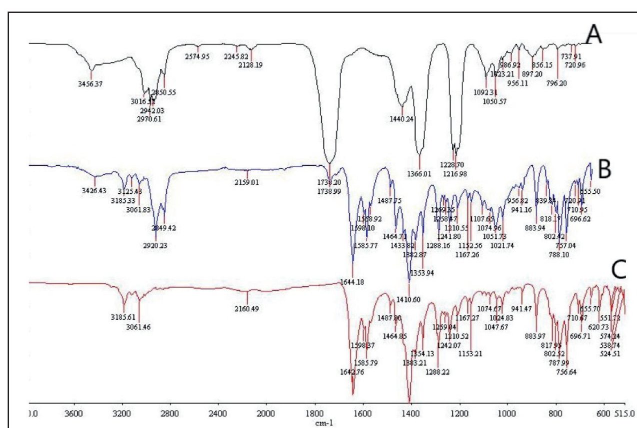

Fig. 7: FTIR spectra of (A) NVP, (B) NVP loaded niosomes and (C) empty niosomes

The spectra (A) and (B) reveal the presence of characteristic N-H and C-N stretching of the 7-membered ring at wavenumbers between 3295 and 3188 cm^{-1} and a C-O stretching vibration for a cyclic amide at 1646 cm^{-1} that are indicative of the presence of NVP (Sarkar et al. 2008). Chemical interactions of NVP would result in complete disappearance of these key signal frequencies. Therefore, no molecular transformation occurred during the formulation and manufacturing process. The spectrum for niosomes without NVP (C) does not reveal the presence of signals for NVP peaks but do show the characteristic signals for cholesterol and DCP.

The entrapment efficiency for NVP in Span® 20 niosomes determined after annealing was 96.8±1.22 %. The niosomes manufactured using Span® 80 exhibited an entrapment efficiency of 98.0±1.86 %. The niosomes formed using Span® 80 exhibit a higher entrapment efficiency relative to Span® 20 niosomes since the HLB value of Span® 80 is lower than that of Span® 20 therefore encapsulating more NVP, as surfactants with low HLB balances entrap hydrophobic drugs more efficiently 1994).

The release of NVP from niosomes of different surfactant composition and free NVP was investigated using the same conditions and these data are depicted in Fig. 8.

Fitting of NVP release data to mathematical models revealed that the release of NVP from Span® 20 and Span® 80 niosomes followed Higuchi release kinetics, exhibiting an R^2 of 0.9974 and 0.9932 respectively implying that release of NVP from niosomes was diffusion-controlled. Relative to free API the rate and extent of release of NVP from the niosomes is retarded indicating prolonged delivery of the API.

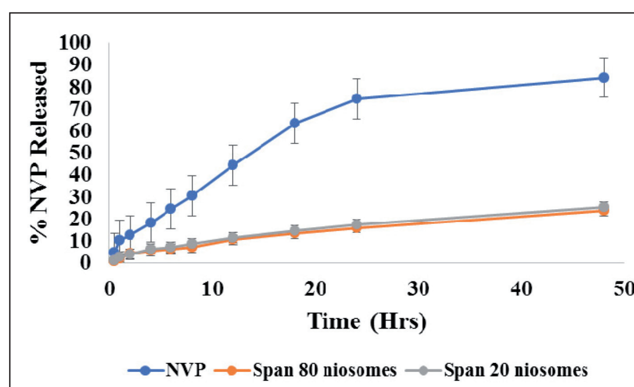

Fig. 8: Comparative release of NVP from Span® 20 and Span® 80 niosomes

2.2.2. *Stability testing*

Stability testing of niosomes was conducted at 4 °C and 22 °C and revealed the niosomes are stable with greater stability observed when stored at 4 °C as at low temperatures fewer collisions between niosomes and these data are summarized in Table 6.

Table 6: Summary of 12-week stability data for optimized niosomes stored in suspension

CQA	Storage condition							
	Span® 20				Span® 80			
	4 °C		22 °C		4 °C		22 °C	
	Prior	After	Prior	After	Prior	After	Prior	After
ZP (mV)	-73.8	-70.0	-73.8	-68.4	-70.9	-69.1	-70.9	-66.2
PS (nm)	572.3	579.2	572.3	610.2	522.6	528.9	522.6	577.72
PDI	0.260	0.420	0.260	0.430	0.200	0.380	0.200	0.410

2.3. *Conclusions*

The thin film hydration technique was successfully used to manufacture NVP Span® 20 and Span® 80 niosomes. Cholesterol and DCP were used as a bilayer stabilizer and charge inducer, respectively. A Box-Behnken Design (BBD) was used to deduce the optimum operating production conditions, *viz.* 100 rpm and 45 min rotation time. In order to avoid repetition NVP Span® 20 niosomes were selected as a discussion topic to describe the optimization approach.

The PS was found to be directly affected by the presence of cholesterol in the formulation. Cholesterol diminishes the liquid-gel transition of surfactant and fits into the spaces between the individual surfactant amphiphile. The PS was also affected by surfactant concentration, albeit not significantly.

The PDI was not significantly affected by any of the parameters investigated and showed that the niosomes produced by Thin Film Hydration exhibited a PDI < 0.500 when manufactured using the parameters defined for these experiments.

The EE was dependent only on the presence of cholesterol in the composition and the relationship between EE and cholesterol content was linear. An increase in cholesterol content resulted in a directly proportional increase in EE for NVP. This was important as the EE was a parameter to be maximized in order to reduce the amount of NVP used during manufacture.

NVP release at 48 h was used to assess the sustained release potential of the niosomes. Increasing the cholesterol content reduced the release rate and increased the entrapment efficiency and is a key finding in reducing dosage, frequency of dosing and length of the dosing interval that in turn may enhance patient adherence.

Stability studies were conducted at 4±2 °C and at room temperature (22 °C) to identify factors likely to affect the stability of

niosomes when stored as suspensions or lyophilized powders. Increasing the temperature of storage resulted in aggregation of niosomes, although not to any significant extent when compared to those stored at 4±2 °C. The stability of niosomes was, however, greatest when the niosomes were stored as lyophilized powders. Lyophilized niosomes are not hydrated prior to storage and are therefore not likely to exhibit leakage or aggregation. In addition, in the solid-state, no particulate collisions are likely to occur in contrast to those observed suspension products.

Sustained release NVP niosomes have been successfully developed, optimized and manufactured. With the aid of DSC and XRD, it was revealed that the niosomes and NVP were crystalline in nature, which resulted in an increased stability and prolonged rate of release of NVP. The niosomes have the potential to be used for targeting NVP delivery to HIV reservoirs and may, as a novel drug delivery system, improve patient adherence to therapy by reducing the side effect profile of the compound. In addition, less frequent dosing may be possible. However, further development and assessment of sustained release NVP niosomes produced in these studies is required. Further development of the technology would necessarily include an assessment of the long-term stability of the dosage form in order to establish a shelf life for the optimized formulation. In addition, differential protein adsorption and *in vivo* studies are necessary to establish performance, safety, pharmacokinetic and toxicity profiles *in vivo*, prior to considering commercialisation of this product.

3. Experimental

3.1. Materials

Nevirapine (NVP) was donated by Aspen Pharmacare® (Port Elizabeth, South Africa). Methanol UV cut off 215 nm (MeOH) and acetonitrile 200 far UV Romil-SpS™ Super Purity Solvent (ACN) (HPLC grade for UV) were purchased from Romil® Ltd (Cambridge, United Kingdom). Chloroform AnalaR NORMAPUR was purchased from VWR Prolabo® Chemicals (Pennsylvania, United States of America). Cholesterol and dihexadecyl phosphate (DCP) were purchased from Sigma Aldrich® (St Louis, United States of America). All other reagents were at least of analytical reagent grade and used without further purification.

3.2. Manufacture of NVP niosomes

NVP niosomes were manufactured by Thin Layer Hydration (Azmin et al. 1985; Baillie et al. 1985; Uchegbu and Vyas 1998). A non-rotatable BBD was used to investigate the impact of four formulation and process variables on the Critical Quality Attributes (CQA) of NVP niosomes. The input variables investigated were rotation speed and time of the round-bottomed flask, cholesterol and surfactant content. Preliminary studies revealed that the inclusion of 5 µmol DCP produced particles that were sufficiently charged and exhibited a ZP at the target level and therefore the DCP content was maintained at 5 µmol for all batches produced.

A 40 mg aliquot of NVP was placed into a round bottomed flask and different molar ratios of surfactant, cholesterol and dihexadecyl phosphate (DCP) added. The powder was dissolved using 10 ml chloroform and methanol in a 9:1 ratio. The solvent was evaporated under vacuum using a Büchi™ R-215 rotary evaporator (Büchi™ Laboratories, Switzerland) for 45 min. Thereafter, the dried lipid layer was hydrated with 10 ml phosphate buffered saline (PBS) at pH 7.4 at 22 °C. Hydration was conducted by rotating the sample at a temperature of 70 °C at a set speed for a specific period as defined by the experimental BBD. Following hydration, the suspension was annealed overnight at 4 °C.

3.3. Characterization of niosomes

Prior to characterisation of the manufactured niosomes, separation of unentrapped NVP was necessary to avoid sample contamination and skewing of results and this approach was undertaken for all characterisations unless otherwise stated. The separation of NVP niosomes from free NVP was achieved using centrifugation. Samples of niosome suspensions were centrifuged at 14000 x g for one hour using an Eppendorf 3154-C centrifuge (Hamburg, Germany). The supernatant was removed using a Pasteur pipette and the niosome pellet washed with PBS and centrifuged for a further one hour to ensure all free NVP was removed from the sample.

3.3.1. Differential scanning calorimetry (DSC)

Approximately 4 mg of lyophilised NVP niosome product was placed into an aluminum pan and sealed after which it was placed directly onto the hot stage of the DSC instrument. DSC thermograms were generated using a Model DSC – 6000 PerkinElmer Differential Scanning Calorimeter (Massachusetts, USA) and were analyzed using Pyris™ Manager Software (Massachusetts, USA). Empty aluminium pans were used as reference standards. The temperature of the DSC was monitored using a central processor and a controlled heating rate of 10 °C /min was used for analysis over the temperature range 30-400 °C. All DSC analyses were performed in triplicate under a nitrogen atmosphere purged at a flow rate of 20 ml/min.

3.3.2. X-Ray diffraction (XRD)

X-ray powder diffraction patterns were generated using a Bruker D8 Discover (Massachusetts, USA) diffractometer equipped with a proportional counter, using Cu-Ka radiation (l = 1.5405 Å, nickel filter). The experiment was performed using a voltage of 30 kV and an associated current of 40 mA. Data were collected using samples on a silicone wafer slide in the range 2θ = 10° to 100°, scanning at 1.5° $min^{-1}$with a filter time-constant of 0.38 s per step and a slit width of 6.0 mm. The X-ray diffraction data were treated using evaluation curve fitting (Eva) software and baseline correction was performed on each diffraction pattern by subtracting a spline function fitted to the curved background.

3.3.3. Particle size analysis

The mean PS and PDI of the niosomes were measured using a Nano-ZS Zetasizer (Worcestershire, United Kingdom) with the instrument set to operate in the PCS mode. Approximately 30 µl of an aqueous dispersion of niosomes was diluted with 10 ml HPLC grade water prior to analysis. The sample was placed in a 10 x 10 x 45 mm polystyrene cell and all measurements were performed in replicate (n=5) at a scattering angle of 90° and temperature of 22 °C. The analysis of PCS data was achieved using Mie theory, with real and imaginary refractive indices set at 1.456 and 0.01, respectively.

3.3.4. Zeta potential (ZP)

The ZP of the niosomes was measured using a Nano-ZS Zetasizer (Worcestershire, United Kingdom) with the equipment set in the Laser Doppler Anemometry (LDA) mode. The sample was prepared as described in § 3.3.3 and placed into z-folded capillary cells for the analysis.

3.3.5. Transmission electron microscopy (TEM)

TEM was used to investigate the shape and surface morphology of niosomes in the original aqueous dispersion. A drop of the aqueous niosome dispersion was placed onto a copper grid with a carbon film. The excess liquid was removed using Whatman® 110 filter paper (Maidstone, England) and the sample allowed to dry at room temperature (22 °C) for 24 hours. The sample was visualized using a Zeiss Libra® 99120 TEM (Munich, Germany) at an accelerating voltage of 20kV.

3.3.6. IR Spectroscopy

The IR absorption spectra of NVP niosomes was generated using a Spectrum 100 FT-IR ATR Spectrophotometer (Beaconsfield, United Kingdom). Approximately 2 mg of powder was placed on a diamond crystal and analyzed over the wavenumber range 4000-650 cm^{-1} at a revolution of 4 cm^{-1} and a scanning rate of 75 scans per second.

3.3.7. Entrapment efficiency (EE)

Entrapment efficiency (EE) was determined by centrifuging 1 ml of each suspension using an Eppendorf 3154-C centrifuge (Hamburg, Germany) at 14000 x g for 1 h. The supernatant was analyzed using a validated HPLC method (Witika, 2017) after disrupting the resultant niosome pellet using n-propanol and sonicating for 1 h.

3.3.8. In vitro release

NVP release studies were conducted using a dynamic dialysis technique (Yoshioka et al. 1994; Ruckmani and Sankar 2010). A 2 ml aliquot of the niosome suspension was centrifuged using an Eppendorf 3154-C centrifuge (Hamburg, Germany) at 14000 x g for 1 h. The supernatant was harvested by decanting into a 10 ml A-grade volumetric flask and the pellet washed using Milli-Q water and then centrifuged for a further 30 min at 14000 x g to ensure all free NVP was dissolved and removed. The pellets were hydrated using 10 ml PBS (pH 7.4) and placed into a 10 cm Membra-Cel X100 CLR dialysis tube of MW cut off 14000 Dalton after which the tubing was sealed at both ends. The receptor fluid was 200 ml 50 µM phosphate buffer pH 7.4 that was placed into a 500 ml beaker. The receptor fluid was agitated at 100 rpm using a Lasec® digital hotplate stirrer (Port Elizabeth, South Africa) set to a temperature of 37 °C. The receptor compartment was sealed with aluminium foil to prevent loss of dissolution medium due to evaporation. A 5 ml aliquot of the dissolution fluid (n = 3) was removed at 0.5, 1, 2, 4, 8, 12, 24 and 48 h and analysed using a validated reversed-phase HPLC method (Witika 2017). The receptor fluid was replaced with fresh medium so as to maintain sink conditions. The release of NVP from each niosome formulation was compared to the release of 40 mg of NVP from 10 ml of a 50 µM PBS at pH 7.4 solution placed into a dialysis bag.

Acknowledgements: The authors acknowledge the Rhodes University Research Committee (RBW), The Henderson Scholarship and the Witika family for their financial support. The authors also acknowledge Aspen Pharmacare® Ltd.

Conflict of interest: The authors report no conflict of interest.

References

Azmin MN, Florence AT, Handjani-Vila RM, Stuart JFB, Vanlerberghe G, Whittaker JS (1985) The effect of non-ionic surfactant vesicle (niosome) entrapment on the absorption and distribution of methotrexate in mice. J Pharm Pharmacol 37: 237–242.

Baillie AJ, Florence AT, Hume LR, Muirhead GT, Rogerson A (1985) The preparation and properties of niosomes—non-ionic surfactant vesicles. J Pharm Pharmacol 37: 863–868.

Govender T, Ojewole E, Naidoo P, Mackraj I (2008) Polymeric nanoparticles for enhancing antiretroviral drug therapy. Drug Deliv 15: 493–501.
Gregoriadis G (1995) Engineering liposomes for drug delivery: progress and problems. Trends Biotechnol 13: 527–537.
Gregoriadis G, Davis C (1979) Stability of liposomes invivo and invitro is promoted by their cholesterol content and the presence of blood cells. Biochem Biophys Res Commun 89: 1287–1293.
Hancock BC, Parks M (2000) What is the true solubility advantage for amorphous pharmaceuticals? Pharm Res 17: 397–404.
Luther J, Glesby MJ (2007) Dermatologic adverse effects of antiretroviral Therapy: Recognition and management. Am J Clin Dermatol 8: 221–233.
Mayer LD, Bally MB, Hoppe MJ, Cullis MR (1986) Techniques for encapsulating bioactive agents into liposomes. Chem Phys Lipids 40: 333-345.
Ofotokun I, Chuck SK, Hitti JE (2007) Antiretroviral pharmacokinetic profile: A review of sex differences. Gend Med 4: 106–119.
Ruckmani K, Sankar V (2010). Formulation and optimization of zidovudine niosomes. AAPS PharmSciTech 11: 1119–1127.
Saad MH, Jahan R, Bagul U (2012) Nanopharmaceuticals: a new perspective of drug delivery system. Asian J Biomed Pharm Sci 2: 11–20.
Sarkar M, Perumal OP, Panchagnula R (2008) Solid-state characterization of nevirapine. Indian J Pharm Sci 70: 619–630.
Sezgin-Bayindir Z, Yuksel N (2012) Investigation of formulation variables and excipient interaction on the production of niosomes. AAPS PharmSciTech 13: 826–835.
Shegokar R, Singh KK (2011) Surface modified nevirapine nanosuspensions for viral reservoir targeting: In vitro and in vivo evaluation. Int J Pharm 421: 341–352.
Stern JO, Robinson PA, Love J, Lanes S, Imperiale MS, Mayers DL (2003) A comprehensive hepatic safety analysis of nevirapine in different populations of HIV infected patients. J Acquir Immun Defic Syndr 34 Suppl 1: S21-33.
Torchilin VP (2007) Micellar nanocarriers: pharmaceutical perspectives. Pharm Res 24: 1–16.
Uchegbu IF, Duncan R (1997) Niosomes containing N-(2-hydroxypropyl)methacrylamide copolymer-doxorubicin (PK1): Effect of method of preparation and choice of surfactant on niosome characteristics and a preliminary study of body distribution. Int J Pharm 155: 7–17.
Uchegbu IF, Vyas SP (1998) Non-ionic surfactant based vesicles (niosomes) in drug delivery. Int J Pharm 172: 33–70.
Wilkhu JS, Ouyang D, Kirchmeier MJ, Anderson DE, Perrie Y (2014) Investigating the role of cholesterol in the formation of non-ionic surfactant based bilayer vesicles: Thermal analysis and molecular dynamics. Int J Pharm 461: 331–341.
Witika BA (2017) The Development, Manufacture and Characterisation of Niosomes Intended To Deliver Nevirapine To the Brain. Rhodes University.
Yoshioka T, Sternberg B, Florence AT (1994) Preparation and properties of vesicles (niosomes) of sorbitan monoesters (Span 20, 40, 60 and 80) and a sorbitan triester (Span 85). Int J Pharm 105: 1–6.